EPJ Web of Conferences **17**, 12001 (2011)
DOI: 10.1051/epjconf/20111712001

A region of oblate nuclides centred at Z = 114 and of spherical nuclides centred at the magic nucleus - A possible scenario to understand the production of superheavy elements beyond copernicium

P. Armbruster[1,a]

GSI Helmholzzentrum fuer Schwerionenforschung GmbH, 64291 Darmstadt, Germany

Abstract. The recent experiments at FLNR, Dubna, demonstrated that cross sections to produce SHEs by ^{48}Ca induced reactions on actinide targets increase beyond Z = 111, reach a maximum of 5 pb at Z = 114/115, and fall below the 1 pb-level at Z = 118. A scenario is proposed to understand the findings within the frame of former experimental results of heavy element production and theoretical predictions on the stability of the nuclides concerned. New ingredients introduced are 1) to shift the next proton shell beyond Pb from Z = 114 to Z = 122, 2) the isotopes of elements Z = 112 to Z = 118 are deformed and their nuclei have oblate shapes, and 3) the fission barriers around the next magic nucleus $^{306}122_{184}$ are larger than the neutron separation energies and reach values in the range of 10 MeV. The ascent of the flat top at $^{306}122_{184}$ is described by the proposed scenario, which likewise excludes to reach the doubly closed shell region at the top by today's experimental methods in complete fusion reactions.

1 Closed proton shell shifts away from Z = 114

^{48}Ca-induced fusion reactions on heavy actinide targets have been investigated at the FLNR-Dubna. The discovery of many isotopes and evidence for new superheavy elements (SHEs) Z = 114 to 118 were reported since 2004 and presented in a review [1,2]. For more than 40 years the proton-shell of SHEs has been positioned at Z = 114 [3,4]. The next neutron-shell stayed fixed at N = 184, as predicted by the early shell model [5], whereas recent calculations position the proton shell at Z = 120 or Z = 122 [6,7]. In 2008 [8] I presented an analysis of α-decay chains for pairs of even-even nuclei measured in the FLNR-experiments. These chains give access to Q_α-values between the ground-states of the isotopes involved. The isospin-values $(N-Z)/2$ characterising the chains were 29 and 30 and cover the even elements between Z = 118 and Z = 112. They cross the proposed proton-shell Z = 114 at N = 172 and N = 174 away from the next neutron-shell at N = 184 by 12 and 10 neutrons. Q_α-values in decay-chains decrease steadily descending the chain to smaller Z-values. Passing a shell a jump from higher Q_α-values above the shell to lower values below the shell is well documented in nuclear data tables [9] for the main shells Z = 82, 50. The size of the jump crossing the magic proton-shell becomes smaller going away from the nearest doubly magic nucleus. We will examine by a comparison to the well-established Pb-shell at equivalent distances in the neutron numbers, whether for a shell at Z = 114 a jump should still be observed at a distance of 12 or 10 neutrons. The point of comparison for the Pb-shell is N = 118. The Pb-shell crossed at N = 119 – 116 by the chains passing from Po via Pb to Hg manifests a jump of (1.21±0.02) MeV at the shell-crossing.

The analysis presented in Fig. 1 demonstrates that the Pb-shell is still clearly visible at ^{200}Pb, and a shell closure at Z = 114 should be manifested in the α-chains presented by FLNR. An analysis of the 11 Q_α-values published for the even elements between Z = 118 and Z = 112 was performed. They cover the chains $(N-Z)$ = 58 – 61. The off-shell decays of ^{294}118 and ^{289,287}114 were compared to the on-shell decays from ^{290,293}116 to ^{286,289}114. A shell closure at Z = 114 is seen not only in the Q_α-values, but also in the 2 proton separation energies S_{2p}. The differences between consecutive Q_α-values, δQ_α, and isotonic S_{2p}-values, δS_{2p}, were selected and compared for off-shell and on-shell decays, Fig. 1. A jump at Z = 114 of (0.02 ± 0.05) MeV follows. Within the statistical errors there is no shell gap observed at Z = 114. The potential energy surface (PES) surrounding ^{288,286}114 is smooth. The analysis of the FLNR-experiments does not support a shell at Z = 114 [3,4], which accompanied SHE-research since 1966. The next proton shell is filled at Z > 114.

2 The Interacting Boson Approximation (IBA) - A guideline to nuclear structure and fission barriers of superheavy nuclei

A guideline to nuclear structure of nuclei in their ground state is given by the Interacting Boson Approximation (IBA) [10,11]. As the existence of SHEs is due to the shell corrections of their ground state energies, it is obvious to ask what the IBA-scheme has to teach us about the nuclear structure of superheavy nuclei. Connecting in a chart of nuclides the magic n-rich nuclei, ^{78}Ni, ^{132}Sn, ^{208}Pb, $^{x+184}X_{184}$, a path is defined by the 3 diagonals of 3 rectangles between ^{78}Ni and the doubly closed superheavy nucleus $^{x+184}X_{184}$. Nearly all the n-rich nuclides on the diagonals have been discovered except the last corner stone in the SHE-region.

[a] e-mail: Peter.Armbruster@gsi.de

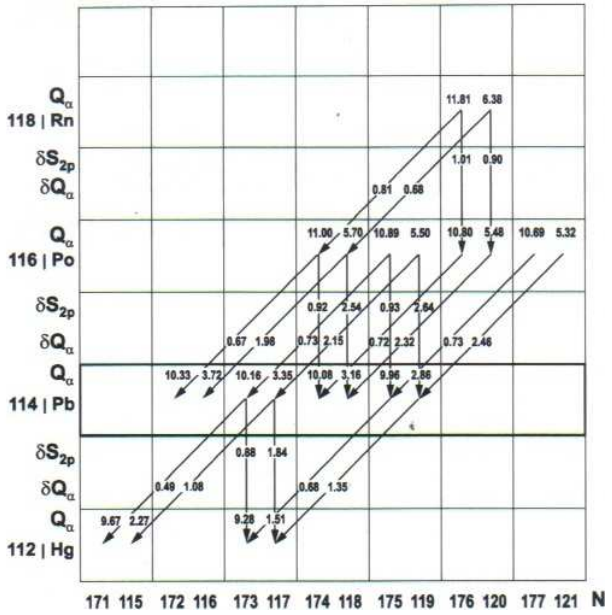

Fig. 1. The jump in the values of Q_α and S_{2p} crossing the shell $Z = 82$ between Po and Pb is analyzed and compared to the corresponding jump at $Z = 114$ between $Z = 116$ and $Z = 114$. Comparing on-shell and off-shell values, the Pb-shell manifests itself in the δQ_α-values, as well as in δS_{2p}-values by an energy difference of $\delta S_{shell} = (1.21 \pm 0.02)$ MeV at the shell crossing. At $Z = 114$ the identical analysis gives for the difference of the δQ_α-values (0.05 ± 0.06) MeV and (-0.02 ± 0.1) MeV for δS_{2p}, respectively. The analysis shows a smooth transition between the Z-values, and no indication of a closed shell at $Z = 114$.

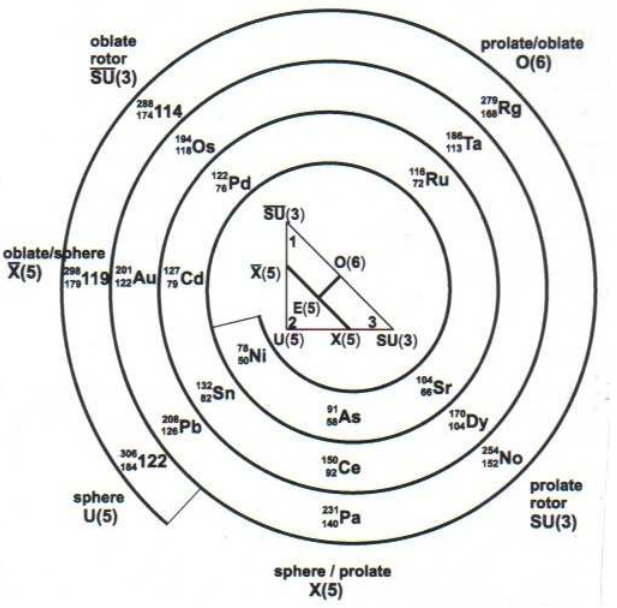

Fig. 2. The Interacting Boson Approximation, as a guide to the understanding of the nuclear structure of deformed and spherical nuclides, is applied to an extrapolation into the regime of SHEs [10]. The triangle in the centre of the figure summarizes the relation between phase-transition points $X(5)$, 0(6), and $\overline{X}(5)$ and the shapes $U(5)$, $SU(3)$, and $\overline{SU}(3)$ [11]. Connecting the double magic nuclei ^{78}Ni, ^{132}Sn, ^{208}Pb, and $^{306}122_{184}$ by 3 straight lines, the nuclei on these lines reveal a periodicity, which is presented by a 3-fold spiral. The nuclear structure up to ^{270}Hs was investigated experimentally, and the IBA-scheme has been applied as an ordering principle. An extrapolation of the prolate-oblate-spherical phase transitions up to the next doubly magic nucleus $^{306}122_{184}$ is proposed here.

The diagonal connects between ^{78}Ni and ^{132}Sn n-rich nuclides, all observed [12], but not well investigated. The second diagonal between ^{132}Sn and ^{208}Pb connects known territory. Especially in its upper part below ^{208}Pb, a region is passed where IBA recently has been applied [13]. The third diagonal between ^{208}Pb and $^{x+184}X_{184}$ covers nuclei with many of them investigated up to ^{270}Hs [14]. The continuation towards the unknown endpoint passes through the isotopes of elements $Z = 112 - 118$ investigated at FLNR, Dubna. The ground state properties of nuclides on the 3 diagonals reveal similarities. Between the magic shell nuclei as corner stones, in the middle of the diagonal we find deformed prolate nuclei ^{104}Sr, ^{170}Dy, and ^{254}No, the deformation parameter β_2 of which shows maximal values. The β_2-value of ^{254}No was measured recently [15, 16] confirming that here half of the way towards the next doubly-closed nucleus has been reached. The extrapolation $^{208}\text{Pb} \rightarrow {}^{254}\text{No}$ gives 122 protons for the last corner-stone. The sub-shell closure $N = 162$ centred around ^{270}Hs was theoretically predicted [17] and a shell strength $S_{shell} = 0.9$ MeV was experimentally determined from decay-chain analysis [18]. This sub-shell closure at $Z = 108$ is situated at 2/3 of the way towards the next doubly closed shell, which is extrapolated at $Z = 121$. The underlying IBA-scheme places the next proton-shell closure well above $Z = 114$. In agreement with recent Hartree-Fock [6, 7] and Relativistic mean field [19] calculations the next closed proton-shell is proposed to be placed at $Z = 122$. The region of spherical nuclei in analogy to the ^{208}Pb-region where it covers the elements between Hg ($Z = 80$) and Po ($Z = 84$), should be expected at $Z = 122 \pm 3$.

The IBA-scheme uses bosons and their symmetries as an ordering principle. The bosons are made of pairs of protons and neutrons, and the symmetries follow from group theory. Three phase transitions, spherical-prolate $X(5)$, prolate-oblate 0(6), and oblate-spherical $\overline{X}(5)$ divide the diagonal in 3 parts. $X(5)$ to 0(6) covers nuclei with prolate deformation $\beta_2 > 0$. Dividing the $\beta_2 > 0$ region in equal thirds, a subdivision is introduced. A maximum of $\beta_4 > 0$ deformations is observed in the centre of the first third, pure $\beta_2 > 0$ is observed in the second third, and $\beta_4 < 0$ deformations are found in the last third of the prolate deformations. All in all half of the nuclei on the diagonal have axially symmetric prolate shapes. $\overline{X}(5)$ to $X(5)$ covers 1/3 of all nuclei on the diagonal. They divide into spherical, all $\beta_i = 0$, and octupole shaped nuclei, $\beta_3 < 0$. The centres of the spherical regions are the magic shell nuclei. In the centre for the $\beta_3 < 0$ - deformed shapes ^{144}Ba and ^{222}Ra were observed and their β_3-parameter measured. 0(6) to $\overline{X}(5)$ covers 1/6 of all nuclei on the diagonal which shows in its centre nuclei with oblate deformations ($\beta_2 < 0$) like ^{122}Pd and ^{196}Os. Figure 2 presents the periodicity together with the extended IBA-symmetry triangle [11]. The phase-transition points and the centres of spherical and prolately and oblately deformed nuclides are presented.

The next magic nucleus with a proton shell at $Z = 122$ and a neutron shell at $N = 184$, is the nuclide $^{306}122_{184}$. Its shell correction energy predicted in the early calculations [20], as well as in the recent publications [6,7] reaches values of about -10 MeV close to the values obtained for the two lower magic nuclides, ^{132}Sn and ^{208}Pb. The height of the fission barrier of $^{306}122_{184}$, assuming for the underlying PES of the macroscopic nuclei a flat dependence in β-deformation space, equals in size the shell correction energy. A barrier of 10 MeV is well above the neutron separation energy.

Nuclear structure contributes to the height of the fission barrier - for SHE in its total - and introduces a difference in the level density for spherical and deformed nuclei - the enhancement of level densities by states of collective degrees of freedom. It is well established by several experiments at GSI [21–23] that collective enhancement of level densities reduces the expected increase of survival probability in nuclei with fission barriers enhanced by shell correction energies for $N = 126$. For deformed nuclei, as for $Z = 112 - 118$, there is no difference in the density of collective states modifying Γ_n and Γ_f. The survival probability actually will approach 1 for $B_f > B_n$. This explains why all decay channels 2n to 5n were observed in the FLNR-experiments to produce isotopes of $Z = 114$ within one order of magnitude in cross section. Traversing the $\overline{X}(5)$ symmetry-point downwards from $Z = 119$, the region of oblate shaped nuclei in analogy to the Os-region below ^{208}Pb is entered. It covers nuclides of the elements $Z = 115 \pm 3$ in the neutron range $N = 174 \pm 4$, centred around ^{289}115. All the isotopes discovered recently at FLNR, Dubna, should have ($\beta_2 < 0$)-deformed oblate shapes. Fission is well investigated for nuclides with prolate shapes. But, little is known about fission of nuclei with spherical shapes, which could be investigated along the $N = 126$ closed shell [24,25]. Never fission of nuclei with oblate shapes was investigated. For the oblate isotopes of SHEs, $Z = 112 - 118$, spontaneous fission was observed in the isotopes ^{286}114 and $^{282-284}$112. This could have been the first observation of fission of oblate nuclides. To pass from an oblate shape over a prolate saddle point towards fission may be a process of reduced probability compared to the fission of nuclides with prolate ground-state deformation. The new superheavy nuclei may have higher stability against fission, which might increase their survival in the deexcitation stage of their formation.

Moving in atomic number upwards towards the doubly closed shell nucleus, finally $^{306}122_{184}$ is accessed. Summarizing the findings of recent SHE- and RMF-calculations there is consensus that the range $Z = 114 - 126$, $N = 172 - 184$ covers a region of low-spin levels [26]. The level densities of the nuclides all in all are reduced. On the contrary, the shell corrections approaching magic nuclei like ^{132}Sn and ^{208}Pb show a peak structure, a steady increase of the slope in the neutron-proton plane until the summit is reached. Not so, in the range of superheavy nuclides. The fission barriers do not span a peak, but a mesa. The slope in the neutron-proton plane starts steep and becomes more and more flat approaching the summit. The fission barriers starting at 3.5 MeV for $Z = 111$ already reach at $Z = 114$ the neutron separation energy $B_n = 6.5$ MeV, at a distance of 3 Z-values. Within the same distance from $Z = 119 - 122$ the increase close to the summit is 1.2 MeV only. Figure 3 presents the fission barriers in a Chart of Nuclides covering the ranges $Z = 101 - 128$ and $N = 150 - 186$. This chart combines two landscapes. Between $Z = 101$ to $Z = 110$ we follow calculations of A. Sobiczewski [17] and R. Smolanczuk [27] describing known territory, and between $Z = 110$ and $Z = 122$ the proposed mesa is shown. The contour lines of fission barrier heights are smoothed. Along the line connecting ^{254}No and ^{306}122 between $Z = 111$ and the summit the contour lines are fixed by the dependence.

$$B_{f(Z)} = B_{f(Z^{min})} + (B_{f(Z^{max})} - B_{f(Z^{min})}) sin\Theta \qquad (1)$$

with $\Theta = \pi/2 \times (Z - Z^{min})/(Z^{max} - Z^{min})$.

A sinΘ-function approaches the path to the mesa. The slope dB_f/dZ follows a cosΘ-function. It is large between $Z = 111$ and $Z = 114$ and approaches zero at $Z = 122$. The line between ^{254}No and the summit ^{306}122 passes the 4 regions discussed in the IBA-scheme with the centres ^{254}No$_{152}$ ($\beta_2 > 0$), ^{270}Hs$_{162}$ (β, -β_4), $^{289}115_{174}$ ($\beta_2 < 0$) and the spherical $^{306}122_{184}$. B_f-values peak at ^{270}Hs and in ^{306}122. A sink at ^{279}Rg is shown at the border line 0(6) between prolate and oblate nuclides. The nuclides produced as evaporation residues (EVR's) in cold and hot fusion reactions are indicated. A heavy line follows the nuclides having lead to element discovery since 1957. Starting by hot fusion (4n,5n), the elements No to Sg were discovered. At $Z = 106$ a change from hot fusion to cold fusion was proposed by Y. Oganessian [28]. By Pb- and Bi-based fusion in 1n-reactions elements Bh to copernicium ($Z = 112$) were synthesized by my former group at GSI, Darmstadt [18,29], and $Z = 113$ was made by Morita *et al.* at RIKEN [30]. A change from cold fusion to ^{48}Ca-induced reactions on actinides was proposed and accomplished again by Y. Oganessian [1] jumping from $^{277}112_{165}$ to $^{283}112_{171}$, a result confirmed in 2007 at GSI [31].

Summarising this section we conclude:

- The isotopes of elements $Z = 115 \pm 3$ are deformed. They are oblate, as their lighter partners at $Z = 76 \pm 3$ and $Z = 46 \pm 2$. Besides the well-known regions around ^{122}Pd and ^{196}Os, a new region of oblate nuclides around ^{288}114 is introduced within the IBA-systematics.
- Oblate nuclides ($\beta_2 < 0$) may have smaller fission probabilities than prolate nuclides ($\beta_2 > 0$). Investigations of fission for oblate nuclei are missing and urgently recommended.
- The prediction of large fission barriers of about 10 MeV for the next doubly closed-shell nucleus ^{306}122 following from recent self-consistent calculations is another ingredient of the scenario.
- B_f-values between $Z = 114$ and $Z = 126$ do not define a peak, as observed at ^{208}Pb, but a mesa-like flat top. For the ascent to this mesa increasing fission barriers following a sinus function are used to fix the barrier height at the connection line between the sink at ^{279}Rg and the top at ^{306}122.

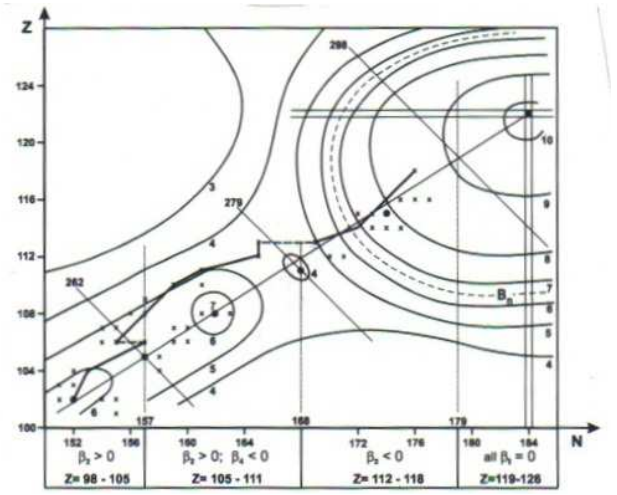

Fig. 3. Fission barriers B_f are presented in a Chart of Nuclides for $N = 152 - 184$ and $Z = 102 - 126$. The contour lines show the height of B_f and $B_n = 6.5$ MeV. The thick line connects the nuclides having served to discover an element. Three production regimes are shown: actinide-based hot fusion reactions ($Z = 102 - 106$), Pb/Bi-based cold fusion reactions ($Z = 107 - 113$), and ^{48}Ca-induced reactions on actinides ($Z = 114 - 118$). The contour-lines are the best approximation to the boundary conditions discussed. No further calculation is underlying this figure.

3 The Production of SHEs and estimates of cross sections

The fusion of two heavy nuclei to produce heavy elements follows a formalism, which is used to describe the process, and which did not change very much since decades, see e.g. Refs.[32,8,18,29]. The cross section is presented by a factor-formula. The factors follow the sequence of stages during the formation process of the fused nucleus.

$$\sigma_{(Z)} = \sigma_{capture} \times p_{(Z)}^{hindrance} \times p^{shape} \times W_{(Z)}^{survival} \qquad (2)$$

$\sigma_{capture}$ is the cross section of two nuclei, which at touching unite to a fused system. It reproduces fusion of lighter nuclei producing non-fissionable EVR's. $\sigma_{capture}$ for our case, the production of the heaviest elements, is of the order of 10 mb. The fused compound system is excited, and deexcites by neutron emission or fission. The probability $W_{(Z)}$ to survive fission depends on the partial probabilities Γ_n and Γ_f to deexcite by neutron-emission (survival) or by fission (destruction), on the excitation energy of the compound system E^x, and the number of deexcitation steps until the ground-state of the EVR is reached.

$$W_{(Z)}^{survival} = [1/(1 + \Gamma_f/\Gamma_n)]^{\nu} \qquad (3)$$

The ratio Γ_n/Γ_f, given an excitation energy E^x and temperature T, depends on the ratio of level densities above the neutron separation energy B_n and the fission barrier B_f.

$$\Gamma_n/\Gamma_f = K \times exp[-(B_n - B_f)/T] \qquad (4)$$

with $K = 1.4 \times A^{2/3}T$, and A, the mass number of the compound system.

$\sigma_{capture}$ and $W_{(Z)}$ allowed for a presentation of fusion induced by α-particles and light ions on actinide-targets. Elements up to $Z = 93 - 106$ were synthesized and correctly described. The production of SHEs in nearly symmetric collision systems for $E^x \sim 0$ and for $B_f > B_n$ seemed possible without fission losses, that is by capture alone at $W_(Z) \rightarrow 1$. Thus, first estimates in 1966 to produce SHEs gave cross sections of 100 mb [32]. These were the times when elements Rf and Db were discovered, and SHE-synthesis became a major goal of nuclear science.

In investigations at GSI of mass symmetric fusion processes aiming at compound systems $Z = 80 - 90$ [33], and of Pb/Bi-based 1n-reactions producing heavy elements in the range of $Z = 102 - 112$ [18,29], cross sections were found to decrease exponentially with increasing atomic numbers. Recently also for ^{238}U-based fusion reactions aiming at $Z = 100 - 108$, the exponential decay was confirmed [34]. The exponential slope was found independent from mass asymmetry. The cross section drops by a factor of 10 increasing the atomic number by two units. The transition between the tow-body system at the point of nuclear capture and the one-body system forming a compound nucleus is highly hindered. The diffusion-like process overcoming the distance of about 6 fm between the two stages acts against increasing and repelling Coulomb-forces. Recent calculations confirm the exponential decay of the reaction flux going into complete fusion [35,36]. A hindrance factor $p_{(Z)}^{hindrance}$ is formulated from the finding $\log(dp^{hindrance}/dZ) = -0.5$.

$$p_{(Z)}^{hindrance} = C \times exp[-0.5/loge \times (Z - Z_0)] \qquad (5)$$

We assume that eq. (5) is valid for all mass asymmetries of the collision systems. The establishment of the exponential hindrance of fusion started at the time of the first SHIP-experiments, and was safely corroborated in ours and others experiments later. In the following discussion nothing is changed in the concept of hindrance formulated in eq. (5).

The factor p^{shape} in eq. (2) remains to be discussed. Here the dependence of the fission probabilities on the shape of the nuclei to be produced is taken into account. Nearly everything we learnt on fission concerns nuclei which show prolate deformations in the ground-state and pass over a prolate saddle point towards fission. For all these nuclides p^{shape} is set equal to one. For the oblate nuclides of elements $Z = 112 - 118$ following a possible stabilisation against fission was proposed and argued in sect. 2, which will be taken into account by a common gain factor of 10 for all the oblate isotopes of the elements concerned.

For spherical nuclei collective enhancement of level densities, in sect. 2 discussed as well, reduces the survival of the compound system. The spherical nuclei neighbouring the closed shell $N = 126$ for elements $Z = 87 - 91$ were found in 1979 to show fission probabilities increased by a factor of 100 compared to their deformed neighbours [21]. In the range of SHEs, $Z = 120 - 126$ close to the shell $N = 184$, the same behaviour is expected, and a loss factor 10^{-2} is introduced in p^{shape} for the spherical superheavy nuclei.

The surprising result of the FLNR-experiments is, that elements $Z = 114$ and $Z = 115$ are produced in ^{48}Ca-induced reactions with cross sections in the range up to 5

pb [1]. These are higher than the cross sections to synthesize the lighter elements $Z = 111$ and $Z = 112$ in Pb/Bi-based reactions. Never before was such a steep rise in cross sections going to higher elements observed.

To apply eq. (2) to the production of SHEs, all ingredients were put together. The factors in eq. (2) in the range of concern between $Z = 112$ and $Z = 118$ are partly constant, like $\sigma_{capture}$ and p^{shape}, or decrease like $p^{hindrance}$ exponentially with increasing atomic numbers. It remains the survival factor $W_{(Z)}$, which could make rise the cross sections for isotopes of $Z = 114$ to 5 pb [37]. The increase of p^{shape} by a constant factor in the above range increases the cross section globally, but it will not contribute to the Z-dependence, which is governed by the interplay of $p^{hindrance}_{(Z)}$ and $W_{(Z)}$ alone. We present $\sigma_{(Z)}$ and its Z-dependent factors in eq. (2) using eqs. (3) and (5).

$$\sigma_{(Z)} = C_0 \times exp[-0.5/loge \times (Z - Z^{min})] \times [1/(1 + \Gamma_f/\Gamma_n)]^{\nu} \quad (6)$$

To calculate the slope $d(ln\sigma)/dZ$ Eqs. (1), (4) and (5) are used in the following:

$$\frac{dln\sigma_{(Z)}}{dZ} = -\frac{0.5}{loge} + \frac{\nu}{T}.\frac{\Gamma_f}{\Gamma_f + \Gamma_n}.\frac{dB_{f(Z)}}{dZ} \quad (7)$$

with

$$dB_f/dZ = \pi/2 \times (B_f^{max} - B_f^{min})/(Z^{max} - Z^{min}) \times cos\Theta \quad (8)$$

and Θ as defined in eq. (1).

Discussing eq. (7) we see that cross sections may increase in the case fission barriers increase with the atomic number, $dB_f(Z)/dZ > 1$. The factor $\Gamma_f/(\Gamma_n+\Gamma_f)$ is close to 1 for $B_f < B_n$, and decreases to small values for $B_f > B_n$. To make $\sigma_{(Z)}$ increase for growing atomic numbers, the number of steps ν in the deexcitation cascade should be as high as possible. Experimentally highest cross sections were observed for $\nu = 3, 4$. Higher values of ν are restricted as shell effects are damped exponentially with the excitation energy E^x of the compound system. A damping factor K_D reduces the fission barrier, $B_f^D = K_D.B_f$. K_D relates to E^x by $K_D = exp(-\gamma E^x)$. A.V. Ignatyuk introduced $\gamma^{-1} = 16/3A^{1/3}/(1+1.3A^{-1/3})$ [38]. K_D as a parameter may take values between no damping, $K_D = 1$, and the value as defined in Ref. [38].

To evaluate eqs. (6) and (7) numerically the variables have to be fixed. We have chosen a set, which underlies the evaluation: $Z^{max} = 122$; $B_f^{max} = 10.5$ MeV; $Z^{min} = 111$; $B_f^{min} = 3.5$ MeV; $B_n = 6.5$ MeV; $\overline{T} = 0.96$ MeV; $K_D = 0.7$; $\overline{\nu} = 3.5$; $K = 5.56$.

In Fig. 4 we present the cross section $\sigma_{(Z)}$, linearly and logarithmically as a function of the atomic number Z. An estimate extrapolating the cross sections observed for $^{34}S/^{238}U \rightarrow {}^{267}Hs$ (5n channel) [39] and $^{26}Mg/^{248}Cm \rightarrow {}^{270}Hs$ (4n channel) [14] to ^{279}Rg gives a cross section of about 50 fb, which was taken as normalisation. The open constant C_0 in eq. (6) for $K_D = 0.7$ was fixed to a value of 380. In Fig. 4, left panel, observed σ-values at FLNR, Dubna, are given for comparison [1]. The isotopes of elements $Z = 112 - 116, 118$ with the largest σ-values are

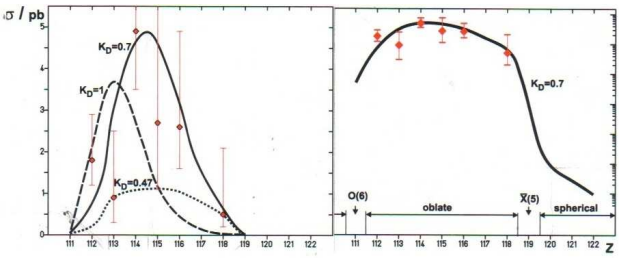

Fig. 4. Left: Production cross sections $\sigma_{(Z)}$ calculated from eq. (2) for a set of variables, as given in the text. Right: $\sigma_{(Z)}$ is shown, as in the left panel ($K_D = 0.7$), but on a log-scale in order to demonstrate the decrease of $\sigma_{(Z)}$ reaching a value of 10^{-5} pb at $Z = 122$.

shown. The rise and fall of $\sigma_{(Z)}$ observed is surprisingly well reproduced. The maximum is stable against a variation of the variables: fission barriers B_f^{max} for $^{306}122_{184}$, the number of steps $\nu = 3$ or $\nu = 4$, and the damping factor $K_D = 0.5 - 1.0$.

The positions of the maxima in $\sigma_{(Z)}$ are restricted to a narrow range of atomic numbers. Fission barriers as a function of Z increasing rapidly in the range $B_f \leq B_n$ reduce the fission losses rapidly and make the survival factor $W_{(Z)}$ increase exponentially. The analogue of this phenomenon stood at the beginning of fission research, the on-set of fission in the element range between radium and uranium. Here, for increasing atomic numbers a rapid on-set of fission was found, and a loss of stability by the new process was established. Now in the range of SHEs not the loss of stability against fission with atomic number is observed, but traversing a small range of fission barriers increasing rapidly with atomic number, the stability against fission grows locally until for $B_f > B_n$ fission disappears. The antipodes of the elements $Z = 112, 114, 116$ are the elements U, Th and Ra. Very small fission losses for elements $Z > 116$ compare to the stability against fission for elements lighter than radium.

In fact having observed the cross section to increase in the range $Z = 111$ to $Z = 115$ conveys the message, that the foot of the ascent to the magic nucleus $^{306}122_{184}$ at the top has been traversed. With $B_f > B_n$ $Z = 118$ was reached at $\sigma = 0.5$ pb. The driving to higher cross sections is stopped, as Γ_f/Γ_n in eq. (7) is going to small values, and the survival is getting close to one. The spherical nuclides in the range $Z = 120 - 126$ and $N = 180 - 190$ again may become, as their $N = 126$-partners, less stable to fission losses. As discussed, collective enhancement of level densities may destroy them in the deexcitation process. The factor p^{shape} above $Z = 119$ has been set to 10^{-2}, but may still be smaller. Fig. 4, right panel, shows the Z-dependence of $\sigma_{(Z)}$ on a logarithmic scale. Following the discussed scenario, staying within well-known physics, there is no hope to reach the top of the mountain of SHEs. In spite, going beyond the point Y. Oganessian and his team have reached at $Z = 118$ is the new challenge.

Summarising this section, we conclude:

– To describe the cross section a 4-factor formula is used. One of the factors, p^{shape}, introduces nuclear structure. Smaller fission possibilities are given to oblate nuclei,

whereas to spherical nuclei increased probabilities were assigned.
– The interplay of two factors, $p_{(Z)}^{hindrance}$, exponentially falling with atomic number, and the survival factor $W_{(Z)}^{survival}$, steeply increasing in the range $Z = 111 - 115$, governs the Z-dependence of the cross section $\sigma_{(Z)}$: A rise of σ-values for increasing Z-values is found in the range $Z = 111 - 114$, a maximum of production in the range $Z = 114 - 116$, and a steady fall for $Z > 116$. The observed cross section dependence for production of elements $Z = 112$ to 118 could be reproduced.
– The scenario presented encourages continuing to work with more sophisticated models and within the frame of known physics in order to solve the remaining questions of SHE's production.
– I regret that with today's experimental methods and the present concept of element synthesis, as presented here, there is little encouragement to go beyond $Z = 118$.

4 What should be done next ?

– Experiments to determine the atomic numbers of the elements $Z = 114 - 118$, either by chemistry or by characteristic K and L x-ray energies.
– How to enter the region of spherical SHE, and to understand production cross sections for reactions induced by beams beyond ^{48}Ca.
– Fission of oblate nuclei has never been observed. Their fission probabilities should be measured
– γ-spectroscopy in the region of SHE should reveal first excited states. Search for isomers.
– Measurements of ground-state binding energies of SHE.
– Search for SHE in the heaviest, binary break-up reactions.
– Not to use consecutive explosions of nuclear weapons to produce by multiple capture reactions large quantities of SHEs.

Acknowledgements

Discussions with K. Duellmann, F.P. Hessberger, M. Schaedel, and M. Stoyer are gratefully acknowledged. Ch. Schmitt, GANIL, helped to shape the manuscript into a publication. Without her help, 15 years after my retirement, I could not have finished this paper.

References

1. Y.T. Oganessian *et. al.*, J. Nucl. and Part. Phys. **G 34** (2007) R165.
2. Y.T. Oganessian *et al.*, Phys. Rev. Lett. **104** (2010) 142502.
3. H. Meldner, Ark. Fys. **36** (1967) 593.
4. A. Sobiczewski *et al.*, Phys. Lett. **22** (1966) 500.
5. M. Goeppert-Mayer and H.D. Jensen, "Elementary Theory of Nuclear Structure", New York, NY, Wiley (1955).
6. J.F. Berger *et al.*, Nucl. Phys. **A 685** (2001) 1c.
7. M. Bender *et al.*, Phys. Lett. **B 515** (2001) 42.
8. P. Armbruster, Eur. Phys. J. **A** (2008), doi 10.1140/epja/i2008-10607-5.
9. G. Audi *et al.*, Nucl. Phys. **A 729** (2003) 1.
10. F. Jachello, Phys. Rev. Lett. **87** (2001) 052502.
11. R. Casten, Eur. Phys. J. **A 20** (2004) 167.
12. M. Bernas *et al.*, Phys. Lett. **B 415** (1997) 111.
13. J. Jolie *et al.*, Phys. Rev. Lett. **87** (2000) 162501.
14. J. Dvorak *et al.*, Phys. Rev. Lett. **97** (2006) 242502.
15. P. Reiter *et al.*, Phys. Rev. Lett. **82** (1999) 809.
16. M. Leino *et al.*, Eur. Phys. J. **A 6** (1999) 63.
17. A. Sobiczewski *et al.*, Phys. Lett. **B 186** (1987) 6.
18. P. Armbruster, Ann. Rev. Nucl. Part. Sci. **50** (2000) 411.
19. P. Ring, Prog. Part. Nucl. Phys. **37** (1996) 193.
20. J.R. Nix, Ann. Rev. Nucl. Part. Sci. **22** (1972) 65.
21. K.H Schmidt *et al.*, Phys. and Chem. of Fission (IAEA), Vienna, Vol. 1, p.409 (1980).
22. A.R. Junghans *et al.*, Nucl. Phys. **A 629** (1998) 635.
23. A. Heinz *et al.*, Nucl. Phys. **A 713** (2003) 3.
24. K.H. Schmidt *et al.*, Nucl. Phys. **A 665** (2000) 221.
25. C. Schmitt *et al.*, Phys. Rev Lett. **99** (2007) 042701.
26. M. Bender, P.H. Heenen and P.G. Reinhard, Rev. Mod. Phys. **75** (2003) 121.
27. R. Smolanczuk, Phys. Rev. **C 56** (1997) 812.
28. Y.T. Oganessian *et al.*, Nucl. Phys. **A 239** (1975) 353.
29. P. Armbruster, Ann. Rev. Nucl. Part. Sci. **35** (1985) 135.
30. K. Morita *et al.*, J. Phys. Soc. Japan **73** (2004) 2593.
31. S. Hofmann *et al.*, Eur. Phys. J. **A 32** (2007) 251.
32. T. Sikkeland, Ark. Fys. **36** (1967) 539.
33. K.H. Schmidt and W. Morawek, Rep. Progr. Phys. **54** (1991) 949.
34. K.E. Gregorich *et al.*, LBNL-Report **63617** (2007).
35. W. Swiatecki, K. Siwek-Wilczynska and J. Wilczynski, Phys. Rev. **C 71** (2005) 014602.
36. Y. Aritomo and M. Ohta, Nucl. Phys. **A 764** (2006) 149.
37. Y.T. Oganessian *et al.*, Phys. Rev. **C 70** (2004) 064609.
38. A.V. Ignatyuk *et al.*, Sov. J. Nucl. Phys. **21** (1975) 612.
39. Y.A. Lazarev *et al.*, Phys. Rev. Lett. **75** (1995) 1903.